
Field-assisted doublon manipulation in the Hubbard model. A quantum doublon ratchet

K. BALZER and M. ECKSTEIN

Max Planck Research Department for Structural Dynamics - University of Hamburg-CFEL, Building 99, Luruper Chaussee 149, 22761 Hamburg, Germany

PACS 71.10.Fd – Lattice fermion models
PACS 71.70.-d – Level splitting and interactions
PACS 37.10.Jk – Atoms in optical lattices

Abstract – For the fermionic Hubbard model at strong coupling, we demonstrate that directional transport of localized doublons (repulsively bound pairs of two particles occupying the same site of the crystal lattice) can be achieved by applying an unbiased ac field of time-asymmetric (sawtooth-like) shape. The mechanism involves a transition to intermediate states of virtually zero double occupation which are reached by splitting the doublon by fields of the order of the Hubbard interaction. The process is discussed on the basis of numerically exact calculations for small clusters, and we apply it to more complex states to manipulate the charge order pattern of one-dimensional systems.

To control and tune macroscopic properties by directly manipulating processes on the atomic scale is an ultimate goal in condensed matter physics. For example, one can selectively excite definite phonon modes [1] and thus create long-lived transients which exhibit interesting properties like superconductivity [2]. The design of suitable mechanisms that support such objectives requires to understand the underlying interplay of strong fields and many-particle interactions, which, nowadays, can be simulated and studied for more and more diverse situations by experiments with ultracold atoms [3–5]. The unprecedented control over the parameters in those systems allows one to explore the crossover between few and many-particle physics [6] and to probe or manipulate systems with single-site resolution [7]. This makes cold atoms well suited to analyze field-induced processes all the way from addressing single particles to complex many-particle states. In extended systems, the impact of an electric field on the correlated particle motion is already nontrivial at weak to moderate interactions (leading, *e.g.*, to damping of Bloch oscillations [8, 9] or nonlinear transport [10]). However, it becomes even more subtle if both the interactions and the field are comparable to or larger than the bandwidth. In this regime, fields can lead to the dielectric breakdown of a Mott insulator [11–13] (which is the many-body analog of the Zener breakdown in band insulators), and when the field and the interaction are resonant, the coupling

of many degenerate states can lead to the emergence of phases which are described in terms of effective spin models [14–16].

In this Letter, we investigate a controlled manipulation of few-particle states based on the interplay of the local repulsive interaction and the external field. We focus on the single-band Fermi-Hubbard model, which is the paradigm model for strongly correlated systems such as cold atoms in optical lattices or interacting electrons in a solid, and we develop a protocol by which an asymmetric alternating (ac) field is used to translate a repulsively bound “doublon” [17] along a chain in a directional motion, reminiscent of a (nondissipative) ratchet [18]. In the case of a *single particle* on a tight binding chain, an unbiased time-periodic driving cannot lead to a finite current or set an initially localized particle into motion, not even when the driving is asymmetric in time and thus breaks time-reversal symmetry [19, 20]. By contrast, the rectification effect in our protocol relies on the *interaction* between the two particles that form the doublon, which will also allow us to use the protocol for a controlled transmutation of more complex states. Moreover, the mechanism can be viewed as a generalization of an optimal control problem which has been discussed for a double quantum dot system [21] and is in line with charge transfer effects in molecules which are exposed to asymmetric laser fields [22].

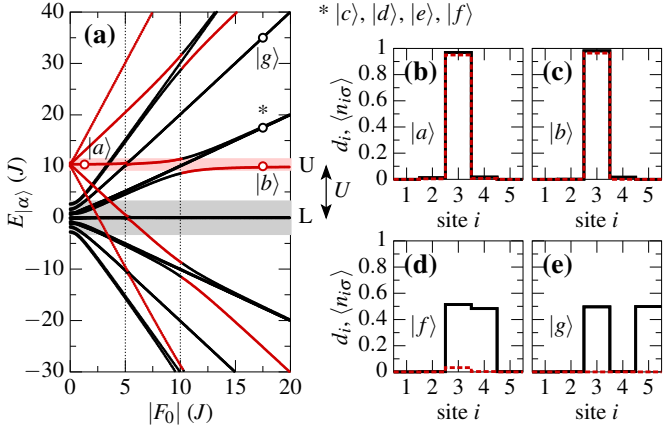


Fig. 1: (a) Stark-shifted energy levels $E_{|\alpha\rangle}$ for two fermions of opposite spin on a five-site chain as function of $|F_0|$ at $U = 10J$. The labels L and U refer to the lower and upper Hubbard bands which strongly overlap at large fields. States with double occupancy $d > 0.5$ [$d = \sum_i d_i = \sum_i \langle n_{i\uparrow} n_{i\downarrow} \rangle$] are plotted in red. Panels (b)-(e) show the densities $\langle n_{i\sigma} \rangle$ (black solid lines) and the local double occupations d_i (red dashed lines) of selected states $|\alpha\rangle$ in (a).

The Hamiltonian is given by

$$H(t) = H_J + H_U + H_F(t), \quad (1)$$

where $H_J = -J \sum_{\langle ij \rangle \sigma} c_{i\sigma}^\dagger c_{j\sigma}$ describes the hopping of fermions with spin σ between nearest-neighbor sites i and j , $H_U = U \sum_i n_{i\uparrow} n_{i\downarrow}$ accounts for the local repulsive interaction, and $H_F(t) = \sum_{i\sigma} \mathbf{F}(t) \cdot \mathbf{r}_i n_{i\sigma}$ is the coupling to an external field $\mathbf{F}(t)$ ($n_{i\sigma} = c_{i\sigma}^\dagger c_{i\sigma}$ is the density, and the lattice spacing is chosen as unit of length, such that fields are measured in units of energy). In the Hubbard model, two particles with opposite spin on the same site form a doublon for sufficiently strong interaction U : For $U > 2W$, where W is the single-particle bandwidth, a single doublon in an otherwise empty lattice can no longer decay into two particles and thus forms a repulsively bound pair [17], which has an infinite lifetime (at zero external field) and an effective hopping amplitude $\propto J^2/U$ [23].

The manipulation of doublons in the field can be understood by analyzing the Stark effect for two particles in a Hubbard chain. Figure 1a shows the Stark-shifted many-particle energy levels for such a system at $U = 10J$, obtained by diagonalizing H for $\mathbf{F}(t) = F_0 \mathbf{e}_x$. At zero field, the strong on-site interaction splits the spectrum into two bands, well separated by an energy gap U . The lower band corresponds to the ‘‘continuum’’ of states with two separated particles (double occupancy $d \ll 1$), while the upper band belongs to the repulsively bound doublon (double occupancy $d \approx 1$). In a finite field F_0 , both bands further split into a Wannier-Stark ladder [24] with states spaced by approximately F_0 (for the lower band) or $2F_0$ (for the upper band). For sufficiently strong fields, the Stark effect thus leads to essential mixing of states of high and low double occupancy. For $J = 0$, the crossing occurs

at characteristic field strengths $|F_0| = U/n$ with integer $n \geq 1$, when the doublon on site i is resonant with two separated particles on sites i and $i+n$ (for $F_0 > 0$) or on sites i and $i-n$ (for $F_0 < 0$). For $J \neq 0$, these resonant levels hybridize and turn into avoided crossings.

In the following, we consider the states labeled $|a\rangle$ to $|g\rangle$ in fig. 1a (F_0 finite). Both states $|a\rangle$ and $|b\rangle$ describe a doublon $|D_3\rangle = |\uparrow_3 \downarrow_3\rangle$ which is localized by the field on the central site 3 of the chain, see figs. 1b and 1c. The states $|c\rangle$ to $|f\rangle$ are very close in energy, become fully degenerate for $|F_0| \rightarrow \infty$ and have low double occupancy. The energetically lowest and highest states in this manifold correspond to the antisymmetric and symmetric superpositions $\frac{1}{\sqrt{2}}(|\uparrow_3 \downarrow_4\rangle - |\downarrow_3 \uparrow_4\rangle)$ and $|S_{34}\rangle = \frac{1}{\sqrt{2}}(|\uparrow_3 \downarrow_4\rangle + |\downarrow_3 \uparrow_4\rangle)$, respectively [see $|f\rangle$ in fig. 1d]. In between we find states of the form $\frac{1}{\sqrt{2}}(|\uparrow_2 \downarrow_5\rangle \pm |\downarrow_2 \uparrow_5\rangle)$ which pass straight through the avoided level crossing at $|F_0| = 10J$. Finally, $|g\rangle$ is the superposition $|S_{35}\rangle = \frac{1}{\sqrt{2}}(|\uparrow_3 \downarrow_5\rangle + |\downarrow_3 \uparrow_5\rangle)$, see fig. 1e, which, like $|f\rangle$, has practically zero double occupancy. Now suppose we prepare the system in the doublon state $|a\rangle$ at a weak field F_0 . If the field is then ramped up to $|F_0| \gg U$ on a fast time scale, the local doublon is preserved, and the system is diabatically transferred into state $|b\rangle$. Contrarily, if the field is turned on smoothly, different final states can be reached depending on which avoided crossing is followed adiabatically. For example, if we quickly pass the crossings at $|F_0| = U/n$ for $n > 1$ and then slowly switch through the resonance at $|F_0| = 10J$ we will end up in state $|S_{34}\rangle$. Similarly we can transfer the system into state $|S_{35}\rangle$ by switching adiabatically around the $n = 2$ crossing at $|F_0| = 5J$ (note that the much narrower crossing requires an essentially slower field tuning in this case).

Including positive and negative fields, a repeated swap between states of the form $|D_i\rangle$ and $|S_{ij}\rangle$ can now be exploited to manipulate doublons in a time-dependent fashion: The field cycle indicated by the green arrows in fig. 2a, *e.g.*, moves a doublon on site 3 (label $|\alpha_i\rangle$) by one lattice spacing to the right (label $|\alpha_f\rangle$). As a definite realization of the cycle we choose a time-dependent field $\mathbf{F}(t) = F(t) \mathbf{e}_x$ of the form

$$F(t) = \begin{cases} F_1 + \gamma(t - t_0^-) & , t_0^- < t \leq t_0 \\ -F_2 + \gamma(t - t_0) & , t_0 < t \leq t_0^+ \\ F_0 & , \text{otherwise} \end{cases}, \quad (2)$$

with $\gamma = (F_2 - F_1)/\Delta t$ and $t_0^\pm = t_0 \pm \Delta t$ (fig. 2b). First, irrelevant level crossings are passed by the sudden change of the electric field from F_0 to F_1 , and the field is ramped linearly (within a time interval Δt) from F_1 to F_2 through the $n = 1$ resonance to split the doublon. Thereafter the field is suddenly reversed (leaving the state invariant), and the process is traversed in opposite manner to restore the doublon on site 4.

In fig. 2b, we numerically validate the field-assisted transport mechanism, time-evolving a doublon which is initially located on the central site of a five-site chain [25]. When the field passes the resonance at $F \equiv U = 10J$

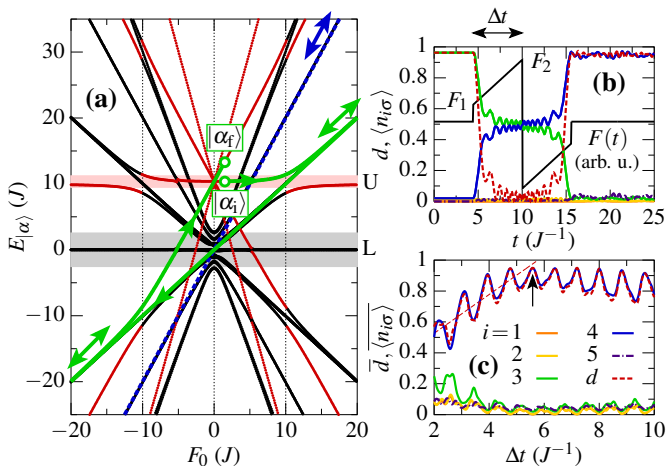


Fig. 2: Doublon manipulation on the linear chain of fig. 1; $U = 10J$. (a) Illustration of the applied field cycle (green arrows). (b) Unitary time evolution of $d(t)$ and $\langle n_{i\sigma} \rangle(t)$ for a doublon initially (at time $t = 0$) prepared on the central site with $F(0) = F_0 = J$. The black line shows the field $F(t)$ shifted in vertical direction and arbitrarily rescaled. In eq. (2), we set $F_1 = 7.5J$, $F_2 = 25J$, $t_0 = 10J^{-1}$ and $\Delta t = 5.584J^{-1}$ (cf. arrow in panel (c)). (c) Dependence of the final values of d and $\langle n_{i\sigma} \rangle$ on the ramp time Δt (values are time-averaged over a period of $10J^{-1}$).

(during the positive part of the field cycle), the double occupancy rapidly drops to $d \approx 0$, and the density becomes equally distributed over sites 3 and 4. Within the negative part of the cycle, the initial double occupancy is recovered, and the doublon emerges shifted on site 4. Figure 2c shows that the resonance must be passed sufficiently slowly ($\Delta t > 5J^{-1}$) to generate the displaced doublon with high fidelity. The oscillations in the fidelity can be explained by Bloch oscillations of the intermediate unpaired state $|S_{34}\rangle$ at frequency $\omega_B(t) = |F(t)|$, which are also visible in fig. 2b. Finally, fig. 3a proves that it is possible, by applying multiple cycles of the form (2), to successively move the doublon site by site through the whole lattice without destroying the spatio-temporal coherence. Note that $F(t)$ has zero time-average, such that any motion of the doublon corresponds to a ratchet-like rectification of the field. Changing the sign of the field cycle will reverse the transport direction.

The feasibility to shift a doublon by two sites in a single field cycle, following the blue path in fig. 2a via the intermediate state $|S_{35}\rangle$ [state $|g\rangle$ in fig. 1e], is shown in figs. 3b-d. As aforementioned, a slower ramp is required to remain adiabatic around the narrower crossing at $F = 5J$ (Δt is about ten times larger), and as a result the intermediate state is subject to stronger decay. However, one can still achieve a final double occupancy of $d \approx 0.8$ with optimal field parameters (red dashed line). With the optimal ramp *successive* motion in steps of two can be realized at least over a few steps although it is much harder than the one-step process, as seen from fig. 3b.

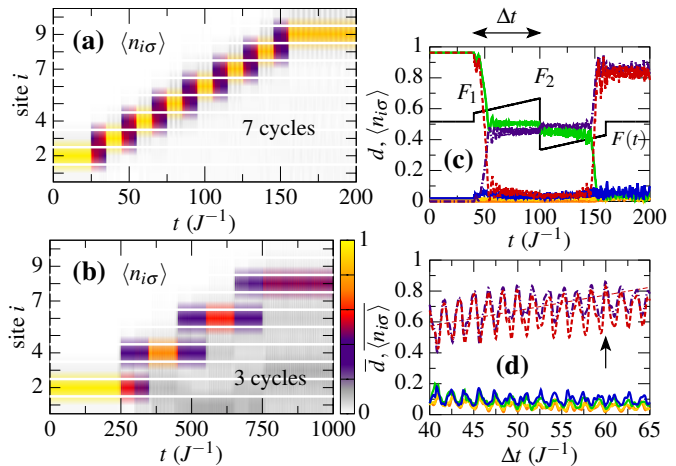


Fig. 3: (a) and (b): Field-assisted directional transport of an initially localized doublon through a one-dimensional chain with ten sites at $U = 10J$ by one site per field cycle (panel (a)) and two sites per field cycle (panel (b)). After seven (three) cycles, the total double occupancy is decreased from 0.96 to 0.87 (0.62) in panel (a) (panel (b)); the field parameters are as in fig. 2b (fig. 3c). (c) and (d): Same as in figs. 2b and 2c but for the translation of the doublon by two sites at a time; parameters: $F_0 = J$, $F_1 = 4.25J$, $F_2 = 10J$ and, in panel (a), $\Delta t = 59.986J^{-1}$.

An interesting question is whether the doublon manipulation protocol can be generalized to higher dimensions. If the field is applied along a principal axis of the lattice, the protocol will not work because particles can delocalize in directions perpendicular to the field. Although the doublon moves only with a reduced hopping J^2/U , the intermediate state of two separated particles can delocalize (independent of U) on a time scale $1/J$ which is not small compared to the traverse of the level crossing. On the other hand, if the field is applied along the lattice diagonal, the transverse doublon and single-particle decay are strongly suppressed because to displace a particle perpendicular to \mathbf{F}_0 one requires two hopping processes against field gradients of $\pm|\mathbf{F}_0|$, *i.e.*, via an off-resonant intermediate state. Figure 4 shows the time evolution during two successive field cycles for a doublon which is initially prepared on the site $\mathbf{r} = (2, 2)$ of a 5×5 square lattice (the parameters $F_{0,1,2}$ are as in fig. 2b and $\Delta t = 3.7J^{-1}$). Obviously, the first cycle, which is centered at $t = 10J^{-1}$, splits the doublon into two equal parts which become located on the next-nearest-neighbor sites (2, 3) and (3, 2). According to this observation, we might expect that additional field cycles lead to further transverse fragmentation, such that the doublon dynamics resembles the classical diffusion dynamics on a Galton board (quincunx) [26] which results in a binomial distribution $B_n(\mathbf{r}_\perp)$ with $n \geq 0$. However, fig. 4 reveals that this picture is not applicable, and quantum interference effects are important: After the second cycle (for $t \gtrsim 35J^{-1}$) we recover a single doublon which is well localized on site (3, 3), cf. the green line. Further-

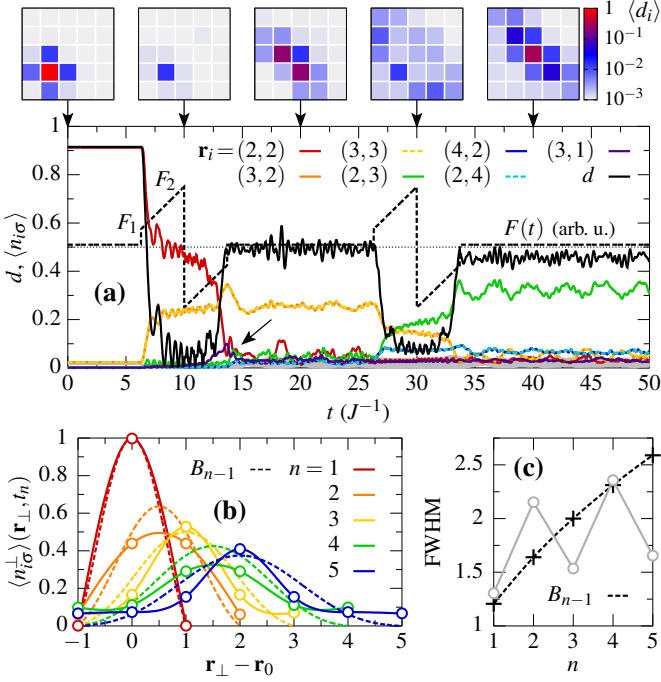


Fig. 4: (a) Doublon transport mechanism applied to a square (5×5) lattice with a doublon initially localized on the site $\mathbf{r} = (2, 2)$; the field $\mathbf{F}(t) = F(t)(\mathbf{e}_x + \mathbf{e}_y)$ [black dashed line] is pointing along the lattice diagonal and $U = 10J$. With exception of $\Delta t = 3.7J^{-1}$ the field parameters are as in fig. 2b. While the colored curves show the time evolution of the particle density $\langle n_{i\sigma} \rangle(t)$ on selected sites \mathbf{r}_i , the black solid line refers to the total double occupancy $d(t)$. The panels above the figure show the spatial distribution of the double occupation at times $t/J^{-1} = 0, 10, 20, 30$ and 40 (plotted on logarithmic scale). (b) Transverse charge distribution $\langle n_{i\sigma}^\perp(\mathbf{r}_\perp, t_n) \rangle$ after cycle n (solid lines) for a calculation, where a single doublon has initially been prepared on the site $\mathbf{r}_0 = (2, 2)$ of a 7×7 cluster. The dashed lines correspond to a binomial distribution $B_{n-1}(\mathbf{r}_\perp)$. (c) Comparison of the full widths at half maximum (FWHM) of the distributions in panel (b).

more, close to 50% of the doublon are lost during the first cycle, while the second cycle almost conserves the total doublon weight.

To better understand the very different nature of the first and second cycle, we separately study the time evolution of states that are present at half the field cycle at times $t = 10J^{-1}$ and $30J^{-1}$, *i.e.*, when the field has just switched sign. Ideally, these states have zero double occupancy and form a triangle abc on the lattice which is either facing into the direction $\mathbf{F}(t)$ (triangle \triangleleft in fig. 5a, intermediate state during the first cycle) or into the opposite direction (triangle \triangleright in fig. 5b, intermediate state during the second cycle). At the avoided crossing $F(t) = -U$, a state with two particles on triangle \triangleleft becomes resonantly coupled by two hoppings with states where particles reside *outside* the triangle (a particle can move from site b to sites 2 or 3 via a resonant doublon state on sites a and c , respectively). A state on triangle \triangleright , on the other hand, is

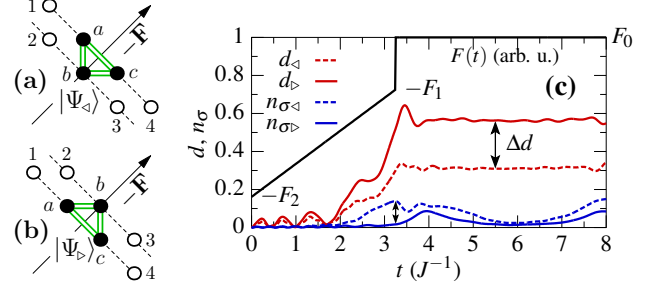


Fig. 5: (a) and (b): Illustration of the states $|\Psi_{\triangleright}\rangle$ and $|\Psi_{\triangleleft}\rangle$ as defined in the text. (c) Time evolution of $d_{\triangleright,\triangleleft}(t)$ and $n_{\sigma\triangleright,\triangleleft}(t)$ in the negative part of the field cycle $F(t)$ (black solid line); the calculations have been performed for an 8×8 cluster with the initial states $\Psi_{\triangleright,\triangleleft}$ prepared in its center. The field parameters $F_{0,1,2}$ are as in fig. 4, $U = 10J$ and $\Delta t = 3.25J^{-1}$.

only coupled resonantly to states *within* the triangle, *i.e.*, the doublon on site b . Hence there is an additional channel for coherence loss when state $|\Psi_{\triangleleft}\rangle$ is moved through the crossing, which is always as dominant as the main process of forming the doublon and can thus not be avoided. As seen from fig. 4, the coherence loss in the first cycle is accompanied by scattering of particles from site $(3, 2)$ to site $(3, 1)$ and equally from $(2, 3)$ to $(1, 3)$ (see the arrow). To further illustrate the effect, we can prepare wave functions $|\Psi_{\triangleright,\triangleleft}\rangle = \frac{1}{\sqrt{6}} \sum_{\mathcal{P}} |0, \uparrow, \downarrow\rangle_{\triangleright,\triangleleft}$, where \mathcal{P} denotes all permutations of the sites a, b and c , and $\langle n_{\sigma\alpha} \rangle_{\triangleright,\triangleleft} = 1/3$ with $\alpha = a, b, c$ (the ket-state is encoded as $|a, b, c\rangle$). During the negative part of the field cycle $F(t)$, the states $|\Psi_{\triangleright}\rangle$ and $|\Psi_{\triangleleft}\rangle$ time evolve as shown in fig. 5c. In particular, we find a difference of a factor of two in the total double occupancies $d_{\triangleright}(t)$ and $d_{\triangleleft}(t)$ for times $t > 4J^{-1}$ which goes along with an early increase of the density $n_{\sigma\triangleleft} = \sum_{\beta} \langle n_{\beta\sigma} \rangle_{\triangleleft}$ at $t \gtrsim 2J^{-1}$ in contrast to $n_{\sigma\triangleright} = \sum_{\beta} \langle n_{\beta\sigma} \rangle_{\triangleright}$ ($\beta = 1, 2, 3, 4$).

In fig. 4b, we extend the analysis of fig. 4a and monitor the transverse charge distribution $\langle n_{i\sigma}^\perp(\mathbf{r}_\perp) \rangle$ [colored solid lines] over more than two field cycles; note that the distributions are time-averaged over a period of $10J^{-1}$ and have been normalized to 1. As discussed above, the diagonal doublon transport occurs in two stages. In the course of this, $\langle n_{i\sigma}^\perp \rangle$ broadens (during odd cycles) and gets compressed (during even cycles). In particular, we find that the degree of compression is such that the transverse decay of the two-particle wave function is smaller than the broadening of a binomial distribution $B_{n-1}(\mathbf{r}_\perp)$, cf. fig. 4c. This again elucidates the quantum nature of the ratchet-like motion.

Because the protocol relies on many-particle interactions, it can potentially be used to transform more complex states among each other. In the final part of this Letter, we use the protocol to transfer a “band-insulating cluster” into a charge-ordered configuration. To this end, we start from a one-dimensional band insulator modeled by a half-filled eight-site Hubbard chain at $U = 20J$ which is initially in the Stark eigenstate $|\Psi_0\rangle = |22220000\rangle$ for

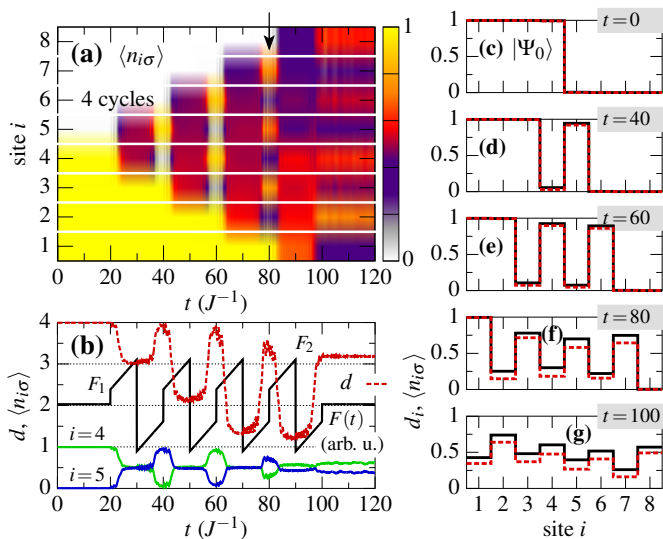


Fig. 6: Field-assisted manipulation of charge order on an eight-site Hubbard chain at $U = 20J$ and half-filling; the number of up and down spins is $N_\sigma = \sum_i \langle n_{i\sigma} \rangle = 4$. (a) Time evolution of the densities $\langle n_{i\sigma} \rangle$ for the system initially (at $t = 0$) prepared in the band insulating state $|22220000\rangle$, cf. panel (c). (b) Time dependence of double occupation and selected densities; the amplitude of the field is indicated by the black solid line. Panels (c)-(g) show the local density $\langle n_{i\sigma} \rangle$ and double occupation d_i for times $t/J^{-1} = 0, 40, 60, 80$ and 100 . The field parameters are $F_0 = J$, $F_1 = 12.5J$, $F_2 = 36J$ and $\Delta t = 10J^{-1}$.

$F_0 = J$, *i.e.*, the first 4 sites are doubly occupied and the remaining sites are empty; the initial double occupation is $d(0) = \sum_i d_i(0) = 4$. In figs. 6a-g, we plot the time evolution of the system following four field cycles $\mathbf{F}(t) = F(t)\mathbf{e}_x$ of the asymmetric form (2), with similar field parameters as before. As one can see, the first cycle displaces only the doublon which is closest to the spatial charge discontinuity whereas all other carriers inside the insulating region (sites 1 to 3) remain Pauli blocked. Therefore, site 4 is almost empty at the onset of the second cycle at time $t = 40J^{-1}$ (fig. 6d), and subsequently two doublons can be moved simultaneously by the field, leaving behind two holes on sites 3 and 5 at $t = 60J^{-1}$ (fig. 6e). Consistently the double occupancy drops temporarily by $\Delta d \approx 2$ during the second cycle. Assisted by the third cycle the initial isolating state is then further transferred into one with alternating charge density but still high double occupancy, see the arrow in fig. 6a. Aside from some minor loss of coherence the state at $t = 80J^{-1}$ is well described by the charge-ordered configuration $|20202020\rangle$, compare with fig. 6f. Finally, the next cycle shifts the whole charge-ordered configuration by one site to $|02020202\rangle$ (fig. 6g) where more than 75% of the initial double occupancy, is preserved for the chosen field parameters; for optimal control parameters and an extended system (where finite size effects become negligible) we expect to observe an even more pronounced signature of this inversion.

In summary, we have studied a quantum ratchet effect

in which doublons in the Hubbard model are moved by unbiased but time-asymmetric electric fields. The effect exploits an adiabatic switching through avoided level crossings in the Stark spectrum (for $U/J \gg 1$) and involves a complete but temporary fragmentation of the doublon at intermediate times. Though adiabaticity is required to avoid dephasing, the mechanism is extremely fast, taking place on time scales comparable to the inverse hopping. The process allows for a directional transport of many doublons simultaneously, and it may be applied to manipulate more complex many-body states. As such, the protocol is interesting from theoretical perspective because it is associated with fast dynamical transitions between states of spatially homogeneous and inhomogeneous charge densities. Fields of the order U can easily be realized for ultracold atoms in optical lattices [27] such that the proposed manipulation scheme may be a good test-ground for experimental setups with single-site resolution. In condensed matter systems, fields corresponding to $F \sim U$ would be extremely large, but related protocols might still play a role for the manipulation of complex states. For example, the shift of the $|20202020\rangle$ configuration which we have demonstrated may be reflected in the rectification of time-asymmetric laser pulses in a charge-ordered medium.

We thank M. GANAHL, for stimulating discussions. Numerical calculations have been performed at the PHYSnet computer cluster at University Hamburg.

REFERENCES

- [1] KAISER S., CLARK S.R., NICOLETTI D., COTUGNO G., TOBEY R.I., DEAN N., LUPI S., OKAMOTO H., HASEGAWA T., JAKSCH D. and CAVALLERI A., *Scientific Reports*, **4** (2014) 3823.
- [2] FAUSTI D., TOBEY R.I., DEAN N., KAISER S., DIENST A., HOFFMANN M.C., PYON S., TAKAYAMA T., TAKAGI H. and CAVALLERI A., *Science*, **331** (2011) 189.
- [3] JORDENS R., STROHMAIER N., GUNTER K., MORITZ H. and ESSLINGER T., *Nature*, **455** (2008) 204.
- [4] BLOCH I., DALIBARD J. and NASCIMBÉNE S., *Nature Physics*, **8** (2012) 267.
- [5] WINDPASSINGER P. and SENGSTOCK K., *Rep. Prog. Phys.*, **76** (2013) 086401.
- [6] WENZ A.N., ZÜRN G., MURMANN S., BROUZOS I., LOMPE T. and JOCHIM S., *Science*, **342** (2013) 6157.
- [7] ENDRES M., CHENEAU M., FUKUHARA T., WEITENBERG C., SCHAUSS P., GROSS C., MAZZA L., BAÑULS M.C., POLLET L., BLOCH I. and KUHR S., *Applied Physics B*, **113** (2013) 27.
- [8] FREERICKS J.K., *Phys. Rev. B*, **77** (2008) 075109.
- [9] ECKSTEIN M. and WERNER P., *Phys. Rev. Lett.*, **107** (2011) 186406.
- [10] OKAMOTO S., *Phys. Rev. Lett.*, **101** (2008) 116807.
- [11] OKA T. and AOKI H., *Phys. Rev. B*, **81** (2010) 033103.
- [12] LENARČIČ Z. and PRELOVŠEK P., *Phys. Rev. Lett.*, **108** (2012) 196401.

- [13] ECKSTEIN M., OKA T. and WERNER P., *Phys. Rev. Lett.*, **105** (2010) 146404.
- [14] SIMON J., BAKR W.S., MA R., TAI M.E., PREISS P.M. and GREINER M., *Nature*, **472** (2011) 307.
- [15] MEINERT F., MARK M.J., KIRILOV E., LAUBER K., WEINMANN P., DALEY A.J. and NÄGERL H.-C., *Phys. Rev. Lett.*, **111** (2013) 053003.
- [16] SACHDEV S., SENGUPTA K. and GIRVIN S.M., *Phys. Rev. B*, **66** (2002) 075128.
- [17] WINKLER K., THALHAMMER G., LANG F., GRIMM R., HECKER DENSCHLAG J., DALEY A.J., KANTIAN A., BÜCHLER H.P. and ZOLLER P., *Nature*, **441** (2006) 853.
- [18] DENISOV S., FLACH S. and HÄNGGI P., arXiv:1311.1086 (2013).
- [19] GOYCHUK I. and HÄNGGI P., *J. Phys. Chem. B*, **105** (2001) 6642.
- [20] PONOMAREV A.V., DENISOV S. and HÄNGGI P., *Phys. Rev. Lett.*, **102** (2009) 230601.
- [21] HELLER E.J., RÄSÄNEN E., BORUNDA M.F. and BLASI T., *Phys. Rev. B*, **87** (2013) 241303.
- [22] TAGLIAMONTI V., CHEN H. and GIBSON G.N., *Phys. Rev. Lett.*, **110** (2013) 073002.
- [23] HOFMANN F. and POTTHOFF M., *Phys. Rev. B*, **85** (2012) 205127.
- [24] WANNIER G.H., *Phys. Rev.*, **117** (1960) 432.
- [25] In order to time evolve the many-body state according to $|\Psi(t)\rangle = U(t,0)|\Psi_0\rangle$ with $U(t',t) = T \exp(-i \int_t^{t'} ds H(s))$ and time-ordering operator T we use the Krylov method.
- [26] GALTON F., *Natural Inheritance* (MacMillan, London) 1889.
- [27] GREINER M., MANDEL O., ESSLINGER T., HÄNSCH T.W. and BLOCH I., *Nature*, **415** (39) 2002.